PRIFYSGOL ABERYSTWYTH UNIVERSITY

Aberystwyth University

A new approach for luminescence dating glaciofluvial deposits - High precision optical dating of cobbles

Duller, G. A. T.; Jenkins, Geraint; Roberts, H. M.; Chiverrell, Richard C.; Glasser, Neil

Published in:
Quaternary Science Reviews

DOI:
10.1016/j.quascirev.2018.05.036

Publication date:
2018

Citation for published version (APA):
Duller, G. A. T., Jenkins, G., Roberts, H. M., Chiverrell, R. C., & Glasser, N. (2018). A new approach for luminescence dating glaciofluvial deposits - High precision optical dating of cobbles. *Quaternary Science Reviews*, *192*, 263-273. https://doi.org/10.1016/j.quascirev.2018.05.036

Document License
CC BY

General rights
Copyright and moral rights for the publications made accessible in the Aberystwyth Research Portal (the Institutional Repository) are retained by the authors and/or other copyright owners and it is a condition of accessing publications that users recognise and abide by the legal requirements associated with these rights.

• Users may download and print one copy of any publication from the Aberystwyth Research Portal for the purpose of private study or research.
• You may not further distribute the material or use it for any profit-making activity or commercial gain
• You may freely distribute the URL identifying the publication in the Aberystwyth Research Portal

Take down policy
If you believe that this document breaches copyright please contact us providing details, and we will remove access to the work immediately and investigate your claim.

tel: +44 1970 62 2400
email: is@aber.ac.uk

Download date: 09. Jul. 2020

Quaternary Science Reviews 192 (2018) 263–273

Contents lists available at ScienceDirect

Quaternary Science Reviews

journal homepage: www.elsevier.com/locate/quascirev

A new approach for luminescence dating glaciofluvial deposits - High precision optical dating of cobbles

G.T.H. Jenkins [a, *], G.A.T. Duller [a], H.M. Roberts [a], R.C. Chiverrell [b], N.F. Glasser [a]

[a] Department of Geography and Earth Sciences, Aberystwyth University, Ceredigion, SY23 3DB, UK
[b] Department of Geography and Planning, University of Liverpool, Liverpool, L69 3BX, UK

ARTICLE INFO

Article history:
Received 6 February 2018
Received in revised form
24 May 2018
Accepted 24 May 2018

Keywords:
Quaternary
Glaciation
Europe
Optical methods
Clasts
Feldspar
Heterogeneous bleaching

ABSTRACT

In recent years luminescence dating has increasingly been applied to date glaciofluvial sediments, but uncertainties about the degree of bleaching of the luminescence signal at deposition make dating of such sediments challenging. Here we test a new approach for luminescence dating of glaciofluvial sediments, based on the analysis of rock cores drilled from granite cobbles, and compare the luminescence ages generated against independent age control.

Luminescence measurements from rock slices in cobble-sized clasts can be used to reconstruct the extent of bleaching, thereby giving greater confidence in the ages produced. This study illustrates that another important advantage of using cobbles is that at depths of 2 mm or more below the cobble surface >90% of the total dose rate arises from the cobble itself, making the dose rate insensitive to the water content of the sediment matrix. Ordinarily, uncertainties in estimating water content during burial are one of the largest sources of uncertainty in luminescence dating methods, and hence reducing the reliance upon the dose rate could be particularly advantageous for glacial deposits, where water contents can potentially be large and highly variable.

Measurements of cobbles from Orrisdale Head, Isle of Man, demonstrate that the luminescence signal was completely bleached to depths of up to 12 mm into the cobble. Sampling of orientated cobbles from lithofacies diagnostic of bar-top environments was used to maximise the chances of exposure to sunlight. The upper-faces of these orientated cobble surfaces appear to be bleached to a greater depth than the lowermost faces. Data from 45 rock slices from these cobbles were tightly clustered, yielding a mean age of 20.7 ± 0.3 ka that is in agreement with independent age control. One of the well-bleached cobbles shows evidence of two discrete exposure events, potentially recording both the advance at 26.2 ± 0.8 ka, and retreat at 20.7 ± 0.3 ka, of the Irish Sea Ice Stream.

© 2018 The Authors. Published by Elsevier Ltd. This is an open access article under the CC BY license (http://creativecommons.org/licenses/by/4.0/).

1. Introduction

Glacigenic sediments are amongst the most challenging Quaternary deposits for dating. Optically stimulated luminescence (OSL) dating using sand-sized grains of quartz or feldspar has been applied in recent years, and whilst many ages have been determined that underpin our understanding of ice sheet dynamics over the last glacial cycle (e.g. Svendsen et al., 2004; Ou et al., 2015; Smedley et al., 2016, 2017a; b), the method is challenging (cf Thomas et al., 2006b; Duller, 2008). In recent years a new luminescence method has been developed, dating buried clasts varying in size from centimetres to tens of centimetres in diameter (Sohbati et al., 2012, 2015; Freiesleben et al., 2015), building upon earlier research (e.g. Habermann et al., 2000; Polikreti et al., 2002; Vafiadou et al., 2007). These clasts are much larger than the sand- and silt-sized grains normally used in luminescence dating (Duller, 2004). One of the benefits of using large clasts for dating is that the degree of bleaching that occurred before burial can be assessed using information encoded within the clast itself (Sohbati et al., 2015). It has also been shown that variations in the luminescence signal with depth into a clast can reveal multiple episodes of bleaching and subsequent burial (Freiesleben et al., 2015). In glacial environments, where heterogeneous bleaching is likely to be a significant problem, the ability to determine whether or not a clast was completely bleached on deposition, prior to subsequent burial, offers a significant advantage over dating sand-sized grains. This is

* Corresponding author.
E-mail address: gej11@aber.ac.uk (G.T.H. Jenkins).

https://doi.org/10.1016/j.quascirev.2018.05.036
0277-3791/© 2018 The Authors. Published by Elsevier Ltd. This is an open access article under the CC BY license (http://creativecommons.org/licenses/by/4.0/).

because when using sand-sized grains, statistical models are required to identify which equivalent dose (D_e) values are derived from sediment grains that were bleached at deposition, and to exclude those that were not bleached (Galbraith et al., 1999). The choice of statistical model, and estimation of parameters such as sigma-b for use in the minimum age model (Galbraith and Roberts, 2012), is complex (Smedley et al., 2017a) and the most appropriate approach is not yet agreed upon.

This study is the first to apply the newly developed cobble dating method to glaciofluvial sedimentary deposits, and aims to see whether it can be used to circumvent many of the issues associated with luminescence dating of sediments in this environment. Critically, the ability of buried clasts to record the extent of bleaching at deposition within a heterogeneously bleached (in this case, glacial) environment will be considered.

2. Materials and methods

2.1. Study area & sample selection

The Orrisdale area, in the north of the Isle of Man, UK (Fig. 1), comprises a complex sequence of ice-front moraines and lateral ice-marginal sandur or outwash systems deposited as the former Irish Sea Ice Stream retreated northwards (Thomas et al., 1985, 2006a; Thrasher et al., 2009). Orrisdale Head was selected because of the extensive (>8 km) exposure in coastal cliff sections and the independent age control available from multiple geochronological techniques in the wider region. The geomorphology around Orrisdale shows a series of repeating packages of proglacial sandur and ice-contact moraine ridges that are also reflected in the coastal exposures (Fig. 1b). Previously, OSL dating constrained the outwash deposits at Orrisdale (Thrasher et al., 2009) to 16.4 to 14.1 ka, but those ages were calculated using the water contents measured at the time of sampling (5–16%) and do not account for water table lowering with coastal cliff retreat (rates typically 1–2 m per year). Recalculating the Thrasher et al. (2009) ages with water contents of 20–23% revises these ages to 18.3 ± 3.5 and 14.2 ± 2.3 ka. Single grain OSL dating of quartz and cosmogenic nuclide dating of the ice retreat sequence in the wider Irish Sea Basin shows ice limits were 500 km to the south on the Isles of Scilly at ~26 ± 1.6 ka (Smedley et al., 2017a), to the south coast of Ireland by 25.1 ± 1.2ka (Small et al., 2018, in press) and pulling back north from Anglesey by 20.3 ± 0.6 ka (Smedley et al., 2017b). Further north, Chiverrell et al. (submitted) have added 11 single grain quartz OSL ages and 8 cosmogenic isotope ages to further define the ice retreat sequence in the northern Irish Sea Basin, and using a Bayesian model were able to constrain deglaciation of the Isle of Man before 18.9 ± 1.0 ka. This chronology is similar to, but refines, previous Bayesian modelling of the ice retreat dynamics (Chiverrell et al., 2013) and also suggests that the small aliquot OSL ages (Thrasher et al., 2009) for the Orrisdale ice marginal complex underestimate the age by 2–6 ka.

Orrisdale Head forms part of an 8 km long coastal section, giving near continuous exposure of glaciofluvial deposits in cliffs up to 30 m in height. At 54.3194°N 4.5727°W a series of gravel bars fining upwards into sand units are seen, and are indicative of deposition in a sandur with repeated packages superimposed upon each other (Fig. 2). Four gravel packages (ORS01, 02, 03, 04) were sampled, lying within 20 m of each other laterally and between ~ 3 and 7 m below the current surface. Stratified planar crossbeds of back-bar gravels (Gp), and massive, clast-supported imbricated bar-top gravel lithofacies (Gm) were targeted for sampling (Fig. 2b and c). These have been interpreted as ice-proximal bar-forms deposited within a dynamic environment of migrating bars and channels (Thomas et al., 1985, 2006a), with the bar-tops potentially emergent above the water, thus maximising the probability that clasts were exposed to daylight before burial.

Forty-five clasts of varying lithologies were obtained from

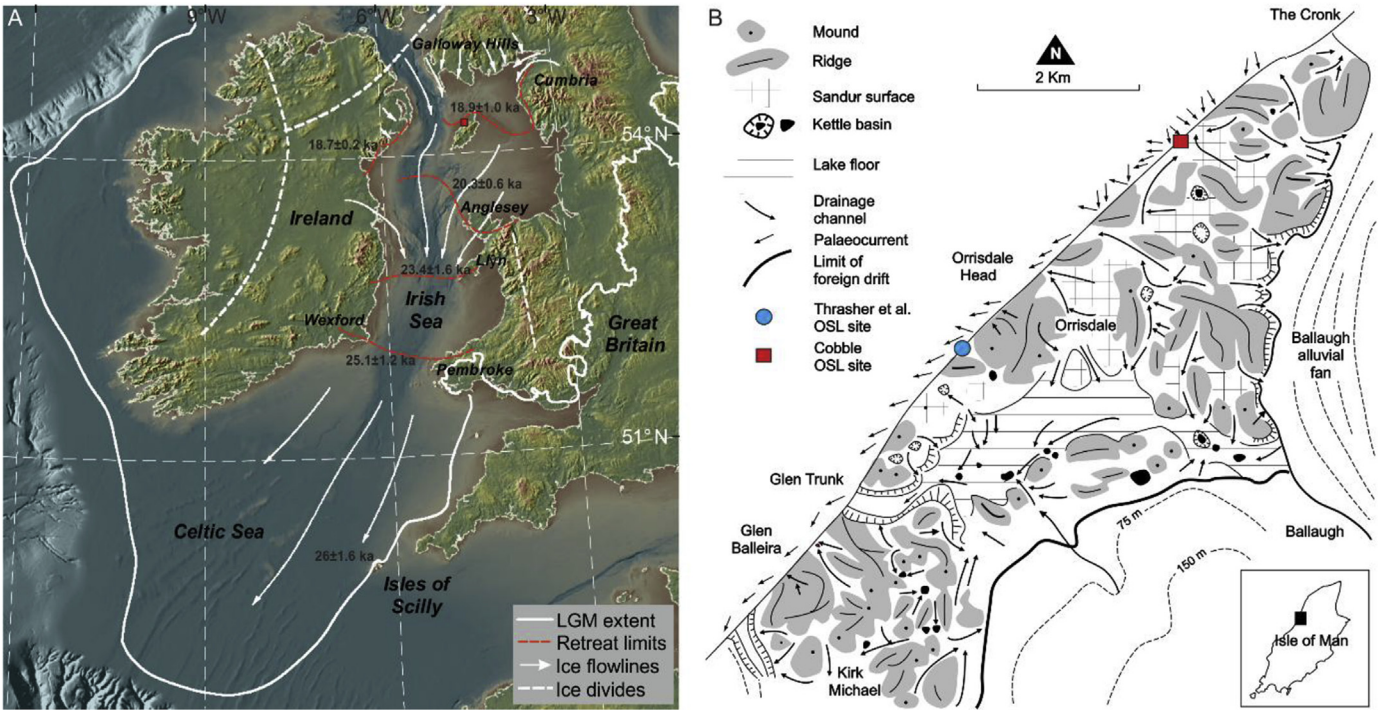

Fig. 1. (a) Location of Orrisdale on the Isle of Man (red square), and its relation to various retreat stages of the Irish Sea Ice Stream and ages for those as discussed in the text. The location of places mentioned in the text are also shown. (b) Geomorphological map of the sandur at Orrisdale Head sampled for this study (shown by a red square). Adapted from Thomas et al. (2006a). (For interpretation of the references to colour in this figure legend, the reader is referred to the Web version of this article.)

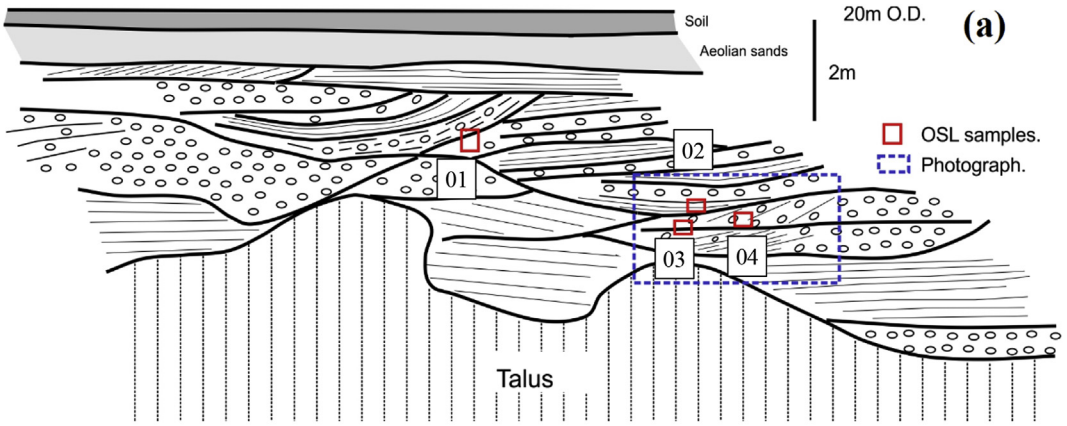

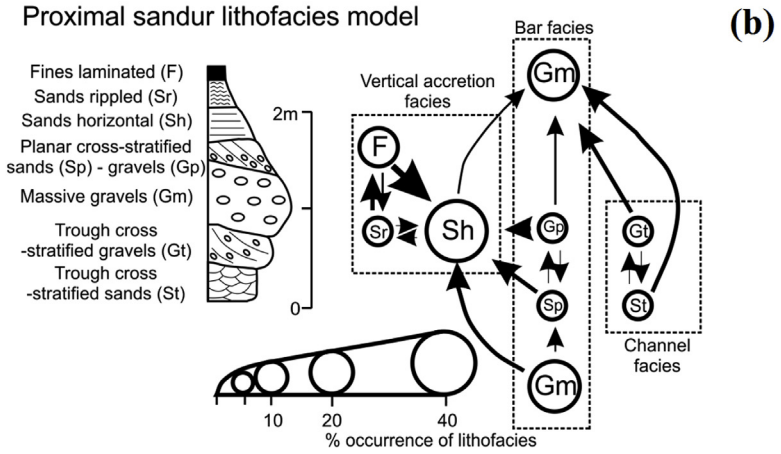

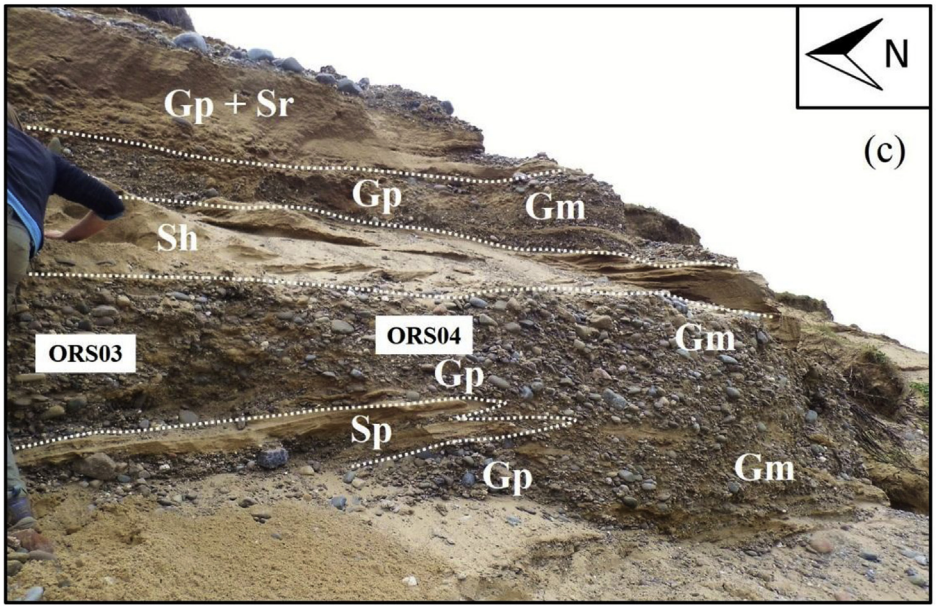

Fig. 2. (a) Schematic of the coastal glaciofluvial sediment exposures at Orrisdale Head with the location of 4 sampled gravel units illustrated (ORS01 - 04). (b) Model of ice-proximal bar formations (Thomas et al., 1985) and key for lithofacies. (c) Example image of the stratified planar cross beds (Gp) and massive, matrix-supported (Gm) gravel lithofacies exposed at Orrisdale Head. The locations where samples ORS03 and ORS04 were collected are also shown.

across the four gravel packages (ORS01 to ORS04). These were collected from sediment exposures which were cleaned and sampled underneath a black, light-tight plastic sheet held against the section to shield the freshly-exposed clasts from daylight. Cobbles with b-axes varying from ~3.5–10 cm were identified within the sediment with the help of a red LED head torch, and collected into light-safe bags. The orientation of each clast within the section was recorded by marking the upper and lower surfaces.

Individual clasts from each package were numbered sequentially to give them a unique name (e.g. ORS03-4 is the fourth cobble from package ORS03). Two samples of the matrix material from each gravel package were also collected for dosimetry, and combined to give a single representative sample of the matrix for each package (samples OH01, 02, 03, 04). The gamma dose rate for each gravel package was also measured in the field by inserting an Ortec Dig-iDART gamma spectrometer equipped with a 2 inch NaI (Tl) crystal into the sediment profile.

2.2. Sample selection, preparation, and measurement protocols

The 45 cobbles sampled were identified in the laboratory as being derived from three lithologies: granites, sandstones and quartz. Following initial investigations, ten granite cobbles were identified as the most appropriate materials for detailed investigation, as the sandstone was too friable to drill and the quartz, thought to be hydrothermal in origin, yielded very little optically stimulated luminescence signal.

Under subdued red light in the laboratory, cores of ~8 mm diameter and of varying lengths (up to ~ 20 mm long) were obtained from the 10 granite cobbles, using a water-cooled, low-speed diamond-tipped drill. Each core drilled from a cobble was given a unique letter code (e.g. core C from ORS03-4 is the third core from cobble ORS03-4). As required, the granite cores were subsequently sliced using a Buehler IsoMet 11–4254 water-cooled, diamond-edged wafering blade (0.3 mm thickness), and rock slices of ~0.7 mm thickness (mean value = 0.71 ± 0.19 mm (n = 116 slices)) were produced. The granite rock slices were washed in distilled water in an ultrasonic bath to remove the rock flour produced during the drilling and slicing process. The clean rock slices were dried and subsequently placed into stainless steel planchettes for luminescence measurements.

All luminescence measurements were made using a Risø TL/OSL-DA-20 reader (Bøtter-Jensen et al., 2003), originally manufactured in 1989 but refurbished with new electronics and a new optical stimulation head in 2010. All measurements, including thermal pretreatments, were carried out in a nitrogen-rich atmosphere. Infrared stimulation (880 nm) was achieved with 22 TSFF5210 LEDs delivering 160 mW/cm^2 at the sample, and photon detection was undertaken with an EMI 9635QA photomultiplier tube filtered by 2 mm thickness each of Schott BG39 and Corning 7–59 filter combined with a neutral density 2.0 filter. A^{90}Sr/^{90}Y beta source mounted on the reader was used for sample irradiation. This beta source was calibrated specifically for rock slices of 0.7 mm thickness, using rock slices from a quartzite cobble sampled from the glaciofluvial sediments at Orrisdale Head. These quartzite rock slices were sensitised and stabilised by giving repeated cycles of irradiation (42.9 Gy) and heating (up to 500 °C), prior to receiving a known gamma dose of 4.90 Gy delivered in a scatter free geometry using a calibrated ^{137}Cs source at DTU, Denmark. The subsequent calibration measurements used the blue-stimulated OSL signal from the gamma-irradiated quartzite rock slices obtained as part of a single-aliquot regenerative dose protocol, and gave a dose rate of 0.031 Gy s^{-1}. This is 82% of the dose rate to sand-sized grains mounted on aluminium discs (but note that the ratio of dose rates will vary depending upon sample-source distance, and this was 11 mm for this instrument).

A post-IR IRSL$_{225}$ SAR protocol based on the approach of Buylaert et al. (2009) was used to study the granite cobble samples from Orrisdale Head (Table 1). To reduce the impact of thermal lag within the ~0.7 mm thick rock slices, a slow heating rate of 1 °C/s was used, coupled with extended preheats held for 100s duration (instead of the more common 60s used when dating sand-sized grains), and the sample was also held at its measurement temperature of 50 °C or 225 °C for 100s before IR stimulation began. A typical decay-curve and dose-response curve for the IRSL$_{50}$ signal are shown in Fig. 3, illustrating the excellent recycling and the intense IRSL$_{50}$ signal typical of the data derived from the granite cobbles in this study.

To assess whether the post-IR IRSL$_{225}$ protocol was appropriate for these samples, two dose-recovery tests were performed on rock slices taken from a single cobble (ORS00-1) collected from the foreshore of Orrisdale Head that had been exposed to daylight for an unknown period of time. In the first dose recovery experiment, the surface slices from each of six cores drilled adjacent to each other on this single cobble were used; three slices were given a beta dose of ~86 Gy on top of their natural D$_e$ prior to measurement of the apparent D$_e$ using the protocol in Table 1. The remaining three slices were used to assess the natural D$_e$ value from the surface of the cobble at the time of sampling, thereby providing a residual D$_e$ value. The resultant residual-subtracted dose recovery values are given in Table 2. The natural D$_e$ ('residual dose', Table 2) derived from the post-IR IRSL$_{225}$ signal is much larger (13.12 ± 1.36 Gy) than that derived from the IRSL$_{50}$ signal (4.36 ± 0.38 Gy). The IRSL$_{50}$ signal recovers the given dose (residual-subtracted dose recovery ratio = 0.97 ± 0.01; Table 2), whilst the post-IR IRSL$_{225}$ signal does not recover the given dose, yielding a residual-subtracted dose recovery ratio of 1.32 ± 0.06 for these naturally-bleached surface-slices (Table 2, Experiment 1).

The second dose recovery experiment used rock slices from the same cores used in dose recovery experiment 1, but taken from deeper into the cobble. Given the relatively high D$_e$ values measured for the surface slices in experiment 1, slices from deeper in the cores were unlikely to have been bleached. For experiment 2, these deeper slices were bleached in a SOL2 solar simulator for 14 days (with the rock slices turned over after 7 days) to reduce the trapped charge population; the same experimental procedure as used in experiment 1 was then applied, with three slices having their apparent D$_e$ measured to provide a residual D$_e$ value, and three slices receiving a dose of 86 Gy prior to D$_e$ determination. The residual D$_e$ values observed following 14 days SOL2 bleaching (1.68 ± 0.17 Gy for the IRSL$_{50}$ signal; 3.38 ± 0.11 Gy for the post-IR IRSL$_{225}$ signal), are significantly lower than observed in the first experiment for natural, sunlight bleaching (60% and 74% lower IRSL$_{50}$ and post-IR IRSL$_{225}$ residuals, respectively). The residual-subtracted dose recovery ratio in experiment 2 is 0.90 ± 0.06 for the IRSL$_{50}$ signal, and 0.97 ± 0.06 for the post-IR IRSL$_{225}$ signal (Table 2).

The IRSL$_{50}$ signal recovered a dose within 10% (allowing for uncertainties) in both experiments (Table 2), whilst the post-IR IRSL$_{225}$ signal only recovered a given dose when the residual signal was lowered by an extended exposure to a solar simulator prior to delivery of the dose to be recovered (Table 2, experiment 2). The reason for this difference in performance is not clear.

3. Dose rate determination

The dose rate to individual rock slices originates from radionuclides in the cobble itself, in the surrounding matrix, and from cosmic rays. A sample of each cobble and a sample of the surrounding matrix were milled to a fine powder prior to dosimetry measurements. Dose rates were determined from thick source alpha counting (TSAC, using a Daybreak 583 instrument) and beta counting datasets (using a Risø GM-25-5 instrument; Bøtter-Jensen and Mejdahl, 1988) (Table 3a). TSAC was used to calculate the U and Th concentrations (Table 3b), and a combination of beta counting and TSAC were used to calculate the K concentration. The U, Th and K concentrations were then combined to establish the external gamma dose rate with the conversion factors of Guérin et al. (2011).

Table 1
Modified Single Aliquot Regenerative dose (SAR) procedure used to measure ~ 0.7 mm thick granite rock slices.

Step	Description	Signal
1	No dose in cycle 1 – different regenerative doses in later cycles	
2	Preheat to 250 °C at 1 °C/s and hold for 100 s	
3	Heat to 50 °C at 1 °C/s, pause for 100 s, and measure IRSL for 200 s	Lx_{50}
4	Heat to 225 °C at 1 °C/s, pause for 100 s, and measure IRSL for 200 s	Lx_{225}
5	Test dose (34 Gy)	
6	Preheat to 250 °C at 1 °C/s and hold for 100 s	
7	Heat to 50 °C at 1 °C/s, pause for 100 s, and measure IRSL for 200 s	Tx_{50}
8	Heat to 225 °C at 1 °C/s, pause for 100 s, and measure IRSL for 200 s	Tx_{225}
9	Heat to 280 °C at 1 °C/s, pause for 100 s, and measure IRSL for 200 s	
10	Repeat cycles 1–9 for different regenerative doses in step 1	

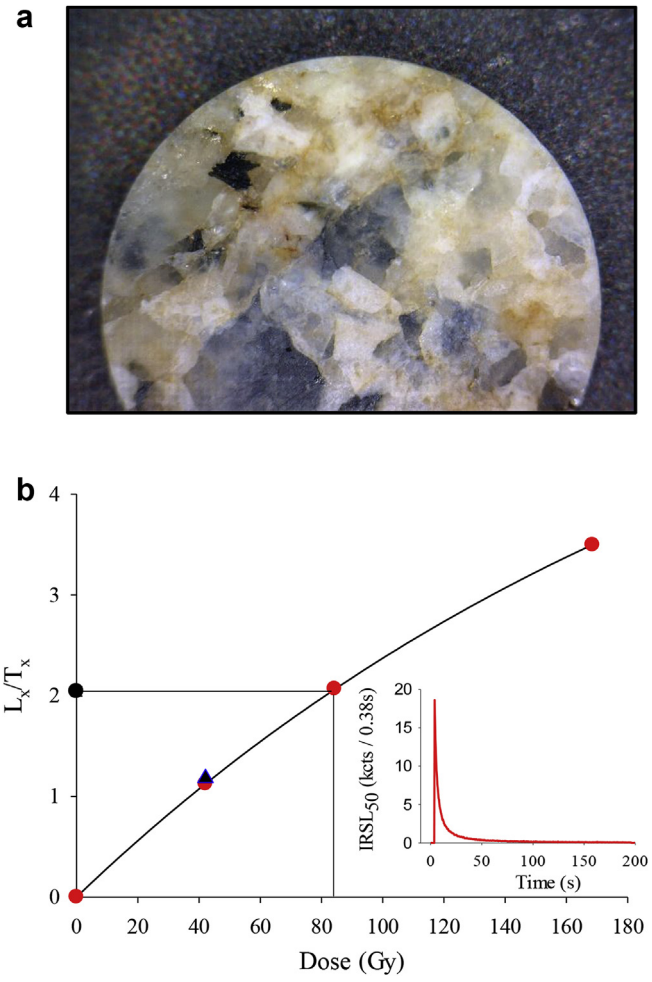

Fig. 3. (a) An example of a rock slice (8 mm diameter) as used for luminescence measurements (from core B of cobble ORS04-1). (b) Dose response curve for the $IRSL_{50}$ signal for the rock slice shown in (a). This slice was from 1.5 to 2.2 mm into the cobble sub-surface. The slice shows excellent recycling (blue triangle). The inset shows the natural decay curve of the same rock slice. For equivalent dose determination, the signal was summed over the first 9 channels (3.4 s) of optical stimulation, and the last 50 channels (19 s) were used to define the background. (For interpretation of the references to colour in this figure legend, the reader is referred to the Web version of this article.)

In-situ measurements of the external gamma contribution (Table 3a) were also made, as described in section 2.1. A water content during burial of 15 ± 5% was estimated for the surrounding sediment matrix, based on saturated water content measurements in the laboratory. In previous studies (e.g. Sohbati et al., 2015) the water content of the cobble itself has been assumed to be negligible. In this study a water content of <0.1% was measured for cobble ORS04–1 demonstrating that the water content is indeed negligible. The internal beta dose rate from K-feldspar grains was calculated assuming a 12.5% K content (Huntley and Baril, 1997). The sizes of feldspar grains within the rock slices were measured using a digital hand-lens and ranged from 320 to 1500 μm and gave a mean value of 647 ± 235 μm. The internal beta dose rate calculated for this grain size was 2.250 ± 0.702 Gy/ka (Table 3a). The dose rate contribution from cosmic radiation was also calculated following Prescott and Hutton (1994).

Freiesleben et al. (2015) calculated the variation of dose rate with depth into a cobble, making use of the approach outlined by Aitken (1985, Appendix H). In Freiesleben et al. (2015), the cobble was part of a rubble layer, and the calculations assumed that the cobble being dated was part of a flat layer, of thickness h and of infinite lateral extent. Equation (1) describes the variation in the beta dose rate with depth (x) into a cobble sub-surface that is buried within a sediment matrix (Freiesleben et al., 2015).

$$\dot{D}(x)_{\beta}^{\text{Cobble}} = \dot{D}_{\text{Rock},\beta}^{\text{inf}}\left[1 - 0.5\left(e^{-bx} + e^{-b(h-x)}\right)\right] + \dot{D}_{\text{Sed},\beta}^{\text{inf}} 0.5\left(e^{-bx} + e^{-b(h-x)}\right). \quad (1)$$

Here, b is the beta attenuation factor (1.9 mm^{-1} following Sohbati et al., 2015) and $\dot{D}_{\text{Rock},\beta}^{\text{inf}}$ and $\dot{D}_{\text{Sed},\beta}^{\text{inf}}$ are the infinite matrix beta dose rates for the cobble and sediment respectively (Table 3a). For cobbles that are typically ~40–90 mm in diameter, the approximation of Freiesleben et al. (2015) is appropriate for the beta dose rate. An equation of the same form is used for the gamma contribution $\dot{D}(x)_{\gamma}^{\text{Cobble}}$ but with an attenuation factor of 0.01 mm^{-1}. For the alpha contribution to the equation $\dot{D}(x)_{\alpha}^{\text{Cobble}}$, the sediment alpha contribution is ignored, due to the short distances (~10 μm) travelled by alpha particles. The alpha contribution arising from the cobble itself is calculated using an a-value of 0.08 ± 0.02 (Rees-Jones, 1995). The dose rate at a specific depth (x) is then calculated by summing the alpha $\dot{D}(x)_{\alpha}^{\text{Cobble}}$, beta $\dot{D}(x)_{\beta}^{\text{Cobble}}$ and gamma $\dot{D}(x)_{\gamma}^{\text{Cobble}}$ contributions, the internal alpha and beta dose, and the cosmic ray dose.

The dose rate to feldspar grains in rock slices in core A from cobble ORS04-1 varies from 5.37 ± 0.72 Gy/ka at the surface to 6.78 ± 0.75 Gy/ka inside the cobble (Fig. 4). The dose rate changes rapidly in the outer 2 mm of the cobble due to the large difference in the beta dose rate from the matrix and the cobble and the limited penetration of beta particles (Fig. 4). The gamma dose varies little, and is much lower (0.31 ± 0.02 Gy/ka at the cobble surface) than the beta dose. At depths of 2 mm or more into the cobble, the internal beta dose arising from K in the feldspar grains is 33% of the total dose rate, and the external beta dose to the grains arising from the

Table 2
Two sets of dose recovery data for slices from cobble ORS00-1 with a given dose approximately equivalent to the expected natural D_e. Cobble ORS00-1 was collected from the modern beach, and assumed to have been bleached to at least some degree due to its location at the time of sampling. Experiment 1 applied the beta dose to be recovered direct to untreated slices prepared from the surface of this cobble, while experiment 2 applied the dose to be recovered to rock slices that had been bleached for 14 days in a SOL2 solar simulator.

	Residual dose (Gy)	Given dose (Gy)	Recovered dose (Gy)	Dose recovery ratio
	Experiment 1: Samples bleached in nature			
$IRSL_{50}$	4.36 ± 0.38	85.86	87.74 ± 0.31	0.97 ± 0.01
pIR $IRSL_{225}$	13.12 ± 1.36	85.86	126.08 ± 5.32	1.32 ± 0.06
	Experiment 2: Sample bleached in a solar simulator			
$IRSL_{50}$	1.68 ± 0.17	85.86	79.01 ± 4.81	0.90 ± 0.06
pIR $IRSL_{225}$	3.38 ± 0.11	85.86	86.44 ± 4.85	0.97 ± 0.06

Table 3a
Measured dosimetry data for cobble and matrix samples from Orrisdale Head. Each individual rock slice will receive a different dose rate as outlined in Section 3.

Attenuated[a] and water corrected dose rates									
Sample name	Sample type	Depth (m)	TSAC[b] (cts/ks/cm^2)	Infinite matrix beta dose rate (Gy/ka)	Beta (Gy/ka)	Gamma (Gy/ka)	In-situ gamma (Gy/ka)	Cosmic (Gy/ka)	Internal beta (Gy/ka)
OH02	Matrix		0.375 ± 0.007	1.383 ± 0.047	0.861 ± 0.079	0.621 ± 0.045	0.687 ± 0.035	–	–
ORS02-1	Cobble	6	1.840 ± 0.032	4.454 ± 0.142	3.292 ± 0.243	3.029 ± 0.200	–	0.104 ± 0.05	2.250 ± 0.702
OH04	Matrix		0.305 ± 0.006	1.257 ± 0.044	0.782 ± 0.072	0.549 ± 0.040	0.799 ± 0.040	–	–
ORS04-1	Cobble	7	1.080 ± 0.019	4.852 ± 0.154	3.586 ± 0.265	2.406 ± 0.131	–	0.094 ± 0.05	2.250 ± 0.702
ORS04-3	Cobble	7	1.460 ± 0.023	5.215 ± 0.166	3.854 ± 0.285	2.643 ± 0.131	–	0.094 ± 0.05	2.250 ± 0.702

Notes.
[a] Beta and gamma dose rates attenuated for grain size within the cobble. Correction for water content is applied to doses arising from the matrix, but not the cobble.
[b] TSAC – Thick-Source Alpha Counting.

Table 3b
Dosimetry data calculated for cobble and matrix samples from Orrisdale Head.

Sample name	Sample type	Cobble Size (mm) (a:b:c)	Depth (m)	K (%)	U (ppm)	Th (ppm)
OH02	Matrix	–		0.62 ± 0.05	1.09 ± 0.18	4.49 ± 0.58
ORS02-1	Cobble	86:57:56	6	3.03 ± 0.20	6.65 ± 1.11	29.66 ± 3.72
OH04	Matrix	–		0.55 ± 0.04	1.33 ± 0.16	4.15 ± 0.52
ORS04-1	Cobble	60:32:30	7	2.41 ± 0.13	4.67 ± 0.60	14.85 ± 2.00
ORS04-3	Cobble	73:39:38	7	2.64 ± 0.13	8.97 ± 0.60	10.76 ± 1.98

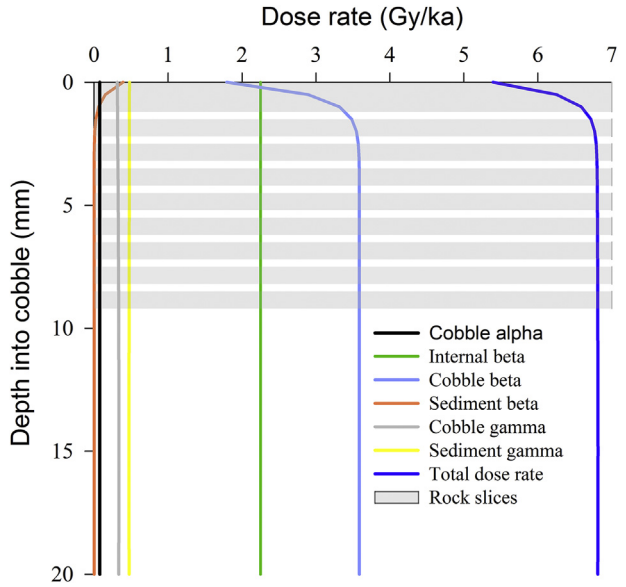

Fig. 4. Dose rate variations with depth into the sub-surface of core A of cobble ORS04-1. The horizontal grey bars show the position of the rock slices, with breaks in these illustrating material lost during the slicing process.

cobble is 53% of the total dose rate. When combined with the gamma dose arising from the cobble itself, this means that 93% of the total dose rate arises from the cobble itself at depths ≥2 mm below the surface. This dose rate is insensitive to the water content of the matrix, and also to potential changes due to post-depositional migration of radionuclides, and hence studying cobbles offers major advantages compared to more conventional dating using sand- or silt-sized sediments. However, care must be taken when assessing the dose rate to the outermost ~2 mm of the cobbles because the dose rate changes rapidly through this upper layer (i.e. the outer 1 or 2 slices in this study, Fig. 4), meaning that small uncertainties in the assessment of the depth will result in large uncertainties in the dose rate (cf. Simkins et al., 2016).

4. Rapid assessment of the degree of bleaching of cobble surfaces

To maximise efficiency, a method was devised to screen cobble samples for suitability for further measurements by rapidly assessing whether or not a cobble face had been exposed to light prior to deposition. This initial screening involved extracting a core of material from each cobble face of interest, and removing a single slice from the surface of each core taken. A total of 23 cores were drilled from 10 cobbles, to assess the variability between different faces of the same cobble, and between cores taken adjacent to each other. The L_n/T_n ratio of these surface slices was determined using

both the $IRSL_{50}$ and post-IR $IRSL_{225}$ signals obtained during a single initial cycle of the SAR measurement procedure shown in Table 1 and using a test dose of ~34 Gy (Fig. 5). As might be expected, the L_n/T_n ratios measured using the $IRSL_{50}$ signals are normally lower than those measured using the post-IR $IRSL_{225}$ signal, both because the $IRSL_{50}$ signal bleaches more rapidly in daylight (e.g. Colarossi et al., 2015), and because the $IRSL_{50}$ signal is expected to suffer from anomalous fading more strongly than the post-IR $IRSL_{225}$ signal (Thomsen et al., 2008).

The 23 L_n/T_n values obtained (Fig. 5) span a wide range from 1.61 ± 0.04 to 9.01 ± 0.19 for the $IRSL_{50}$ signal, presumably reflecting differences in the exposure of the cobbles to daylight at the time when the sandur was deposited. Where two or more cores were taken from the same face of a well-bleached cobble, the L_n/T_n values were consistent for a given signal (e.g. L_n/T_n for $IRSL_{50}$ for core A of ORS04-1 is 1.99 ± 0.04 and for core B of the same cobble is 2.03 ± 0.04). Replicate measurements of unbleached surfaces showed greater scatter (e.g. data for ORS02-1 shown as blue diamonds in Fig. 5); this scatter is also observed when looking at L_n/T_n values for cores where the signal is at saturation (e.g. Fig. 6a). In some instances large differences were observed between different faces of the same cobble (e.g. cobble ORS02-1, Fig. 5), and within the small data set available the upper cobble surfaces were significantly better bleached than the lower cobble surfaces, implying that much of the bleaching of the cobbles occurred after deposition. The data shown in Fig. 5 suggest that the measurement of L_n/T_n ratios from the outer surface of cores removed from a cobble face is sufficient to serve as a rapid, initial screening test to infer the degree of bleaching of the cobbles prior to deposition, and hence to identify the suitability of the core material for further measurements. The validity of this rapid screening test is assessed in Section 5, by selecting a range of natural L_n/T_n ratios identified for surface slices in Fig. 5, and exploring how this signal changes with depth into the cobble.

5. Verifying bleaching by measuring changes in luminescence with depth into the cobble

Following the initial screening to identify those cobbles that were best bleached at deposition (Section 4), the variation in luminescence signal with depth was investigated, to explore whether the inferred pattern of bleaching at deposition had been correctly identified from the measurements of surface L_n/T_n ratios alone (Section 4). The remaining material from ten cores drilled from four of the cobble faces tested in Fig. 5 was sliced and used for this experiment. The cores were selected to span the range of surface L_n/T_n ratios observed in Section 4: duplicate cores were examined for surface slices with low L_n/T_n ratios, taken from the upper face of two different cobbles (cores A and B from cobble ORS04-1, and cores A and B from cobble ORS04-3); three cores were examined from across one cobble face with an intermediate L_n/T_n ratio for the surface slices (cores F, G and H from cobble ORS02-1), and three further cores were examined from the same cobble but taken from the lowermost face, which had a high L_n/T_n ratio for the surface slices (cores C, D and E from ORS02-1). The L_n/T_n ratios with depth into each of these ten cores was investigated, up to a maximum depth of ~25 mm into the cobbles.

Fig. 6a shows the variation in L_n/T_n ratio with depth for both the $IRSL_{50}$ and post-IR $IRSL_{225}$ signals, derived from triplicate cores (C,

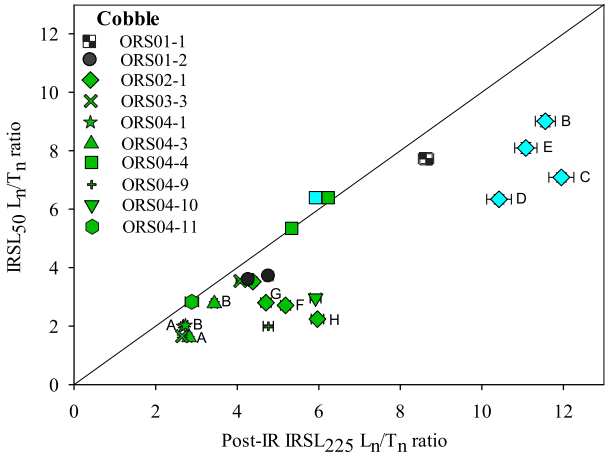

Fig. 5. A comparison of the $IRSL_{50}$ and post-IR $IRSL_{225}$ L_n/T_n ratios for 23 different granite surfaces with the location of the rock slices on the cobbles also illustrated (green – upper-face, black – side-face and blue – bottom-face of the cobbles). Individual cores from cobbles ORS02-1, ORS04-1 and ORS04-3 discussed in the text are labelled with their core letter. The large difference in bleaching from one face of a cobble to another is also illustrated here (see data for different faces of ORS02-1, green and blue diamond symbols). (For interpretation of the references to colour in this figure legend, the reader is referred to the Web version of this article.)

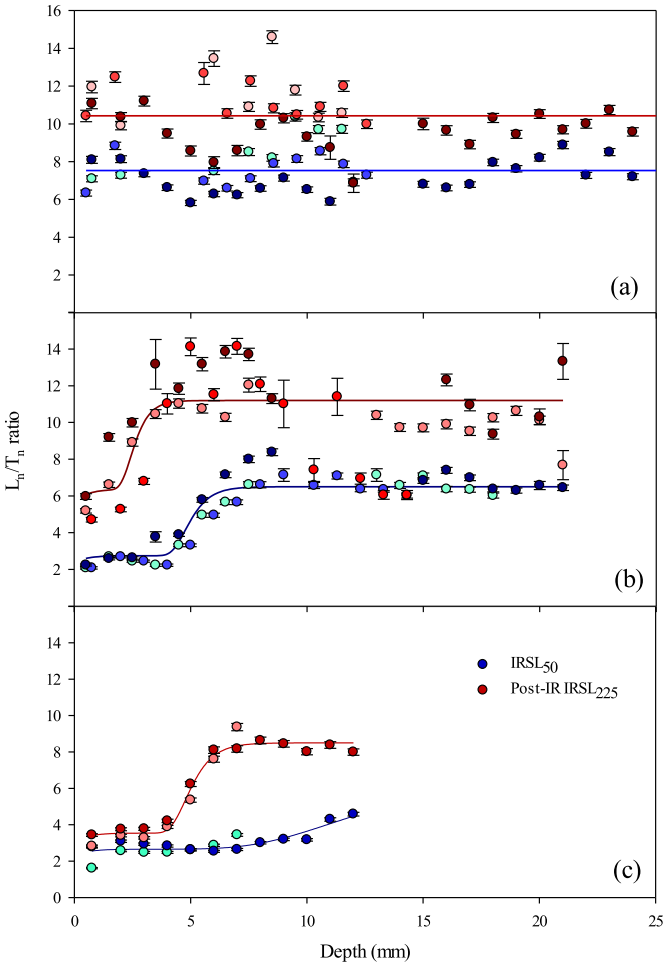

Fig. 6. L_n/T_n ratios for $IRSL_{50}$ (red shaded symbols) and post-IR $IRSL_{225}$ (blue shaded symbols) shown for each individual rock slice, with depth into cobbles with a range of sub-surface characteristics. Triplicate cores from cobble ORS02-1 (cores C, D and E in Fig. 6a, and cores F, G and H in Fig. 6b), and duplicate cores from cobble ORS04-3 (cores A and B, Fig. 6c) were taken, and illustrate similar L_n/T_n ratios with depth for rock slices from different cores. The solid lines in Fig. 6a–c illustrates the fitting of a bleaching model used by Freiesleben et al. (2015) to quantify exposure periods. (For interpretation of the references to colour in this figure legend, the reader is referred to the Web version of this article.)

D and E from ORS02-1), each of which had a high L_n/T_n ratio for the surface slices shown in Fig. 5 (Section 4). There is no obvious trend in the L_n/T_n data for either signal with depth (Fig. 6a), and the L_n/T_n ratios observed are relatively high, which is consistent with neither the $IRSL_{50}$ signal or the post-IR $IRSL_{225}$ signals having been bleached (Fig. 5), as also inferred from examination of the surface slices alone. The laboratory-saturation levels for the $IRSL_{50}$ and post-IR $IRSL_{225}$ signals were assessed for three slices from core E of ORS02-1 using a SAR protocol (Fig. 7), giving an L_x/T_x value of 10.4 ± 0.7 ($n = 3$ slices) for post-IR $IRSL_{225}$ signal saturation in the laboratory, similar to the level observed for the L_n/T_n values through the core (mean value $= 10.4 \pm 1.5$, $n = 3$ slices; Fig. 6a), which is also consistent with the idea that this surface of the cobble was not bleached prior to deposition. The similarity between the L_n/T_n ratio from the natural slices and the laboratory-determined L_x/T_x saturation values, also implies that the post-IR $IRSL_{225}$ signal in this study is not affected by anomalous fading. In contrast, the L_n/T_n values for the $IRSL_{50}$ signal from the same cores (average value 7.53 ± 1.06, $n = 3$ slices; Fig. 6a) are significantly lower than the laboratory-determined L_x/T_x saturation values for the $IRSL_{50}$ signal (11.9 ± 0.7, $n = 3$ slices; Fig. 7), implying that the $IRSL_{50}$ signal is subject to anomalous fading (see section 6).

The change in L_n/T_n ratio with depth for triplicate cores F, G and H from cobble ORS02-1 which had intermediate surface L_n/T_n values (Fig. 5; section 4), are shown in Fig. 6b. The L_n/T_n ratios for both the $IRSL_{50}$ and post-IR $IRSL_{225}$ signals for this face of cobble ORS02-1 (cores F, G and H) are lower than those observed for the un-bleached face of this same cobble, discussed above (cores C, D and E from ORS02-1; Fig. 6a). Additionally, the L_n/T_n values for the $IRSL_{50}$ signal are consistently lower than those from the post-IR $IRSL_{225}$ signal, partly due to the greater bleachability of the $IRSL_{50}$ signal (e.g. as demonstrated by Colarossi et al., 2015), but also likely due to the greater rate of anomalous fading for the $IRSL_{50}$ signal compared to the post-IR $IRSL_{225}$ signal. The enhanced bleachability of the $IRSL_{50}$ signal also results in the $IRSL_{50}$ signal being bleached to a greater depth than the post-IR $IRSL_{225}$ signal. However, at depths below ~7 mm and ~4 mm for $IRSL_{50}$ and post-IR $IRSL_{225}$ signals respectively (cores F, G, H in Fig. 6b), the L_n/T_n ratios are the same as those observed for the face that has not been bleached (cores C, D, and E in Fig. 6a). It is interesting to note that the change in L_n/T_n with depth in Fig. 6b is derived from the same cobble (ORS02-1) as the poorly-bleached cores shown in Fig. 6a, but from a different surface, showing the heterogeneous pattern of bleaching that is possible for a single clast. This emphasises the importance of recording the orientation of clasts on sampling, and considering the geomorphological processes at work prior to deposition.

The two cores (A and B) from cobble ORS04-3 (Fig. 6c) yielded low L_n/T_n ratios at their surfaces (Fig. 5), implying this surface of the cobble had been well-bleached on deposition. Here, both the $IRSL_{50}$ and post-IR $IRSL_{225}$ signals give low L_n/T_n ratios to much greater depths into the cobble sub-surface than for the cobble face considered in Fig. 6b. It is apparent, therefore, that there are significant differences recorded in these bleaching profiles (even for different faces of the same clast c.f. Fig. 6a and b), and the cobble surface in Fig. 6c has been exposed for a longer period of time than either of the surfaces shown in Fig. 6a and b. The bleaching profile in Fig. 6b is in-turn better bleached than that in Fig. 6a. This consideration of the bleaching profiles with depth, indicates that the initial L_n/T_n surface slice analysis effectively identified the well-bleached cobbles within the population at Orrisdale Head. To calculate an age, the data from those cores that show signs of having been bleached were selected, but the extent to which anomalous fading affects the $IRSL_{50}$ and post-IR $IRSL_{225}$ signals needs consideration.

6. Assessment of anomalous fading

Anomalous fading can be a significant issue when dating using feldspars (e.g. Huntley and Lamothe, 2001). The similarity between the laboratory saturation level for the post-IR $IRSL_{225}$ signal (Fig. 7; 10.4 ± 0.7) and the L_n/T_n ratio obtained from an unbleached cobble (Fig. 6a; 10.4 ± 1.5) imply that this signal is not affected by anomalous fading. In contrast, the $IRSL_{50}$ signal does appear to fade, based on the laboratory L_x/T_x versus natural L_n/T_n saturation values (cf. Figs. 7 and 6a). To quantify rates of fading, measurements were undertaken on 20 different granite rock slices, from cores taken from three different clasts (from two well-bleached cobbles (ORS04-1 and ORS04-3) and an exposed cobble from the foreshore of Orrisdale Head (ORS00-1)). Rock slices were irradiated (42.9 Gy) and preheated prior to storage for periods up to 1 month, following the method of Auclair et al. (2003). The average g-values were $2.53 \pm 0.65\%$ per decade ($n = 20$ slices) for the $IRSL_{50}$ signal, and $1.62 \pm 0.69\%$ per decade for the post-IR $IRSL_{225}$ signal ($n = 20$ slices) (Fig. 8). It is interesting to note that the g-value for the post-IR $IRSL_{225}$ signal is not zero, as was implied from the similarity between the natural and laboratory saturation values (Figs. 7 and 6a), although the measured g-value is within uncertainties of a value of

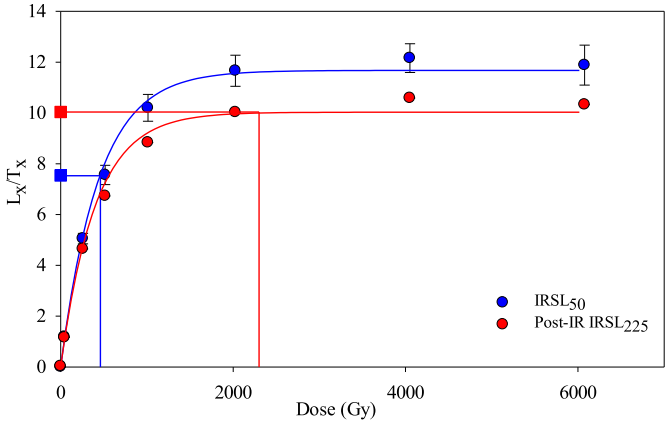

Fig. 7. $IRSL_{50}$ and post-IR $IRSL_{225}$ dose response curves for three rock slices (with each data point the average of these three slices) fitted with a double-saturating exponential equation. The dose-response curves show the saturated laboratory L_x/T_x values and allow comparison to the natural saturated signals (square symbols). The $IRSL_{50}$ signal yields an apparent D_e of 518 ± 40 Gy.

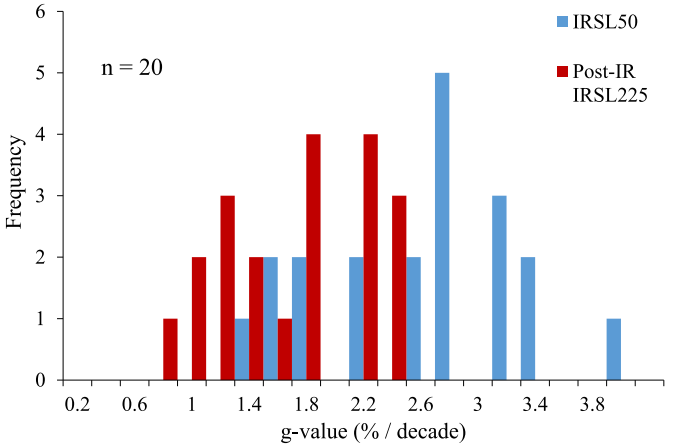

Fig. 8. g-values (%/decade) for both the $IRSL_{50}$ and post-IR $IRSL_{225}$ signals, showing a lower post-IR $IRSL_{225}$ fading value.

1.3 ± 0.3% per decade measured for quartz OSL by Thiel et al. (2011), a signal that is widely accepted not to fade. Both of these measurements illustrate the challenge of making and interpreting fading measurements in the laboratory, particularly where fading rates are low. Given the similarity of the fading rate measured for the post-IR $IRSL_{225}$ signal in this study and the apparent quartz OSL fading rates of Thiel et al. (2011), no correction is made in this study for fading of the post-IR $IRSL_{225}$ signal. The $IRSL_{50}$ age of each slice has been corrected using the method outlined in Huntley and Lamothe (2001) using the average measured fading rate of 2.53 ± 0.65% per decade. As discussed in the next section, even without correcting the post-IR $IRSL_{225}$ ages for fading, they consistently yield older ages than those derived from the $IRSL_{50}$ signal after correcting for fading.

7. Luminescence ages from cobbles and comparison with independent age control

Ages for rock slices from three cobbles are shown in Fig. 9a–c; the post-IR $IRSL_{225}$ ages are not corrected for fading, but the $IRSL_{50}$ ages are corrected as described in section 6. Each data point in Fig. 9 is the average D_e of two, or typically three slices from the same depth on the same clast face, divided by the dose rate for that specific slice-depth calculated following the method described in section 3. Independent age control (18.9 ± 1.0 to 20.3 ± 0.6 ka; Chiverrell et al., submitted; Smedley et al., 2017b) described previously (Section 2.1) is included on Fig. 9 as a light red horizontal bar. To calculate an age for the deposition of each cobble, the ages from different depths into the cobble sub-surface are combined as shown in Fig. 9.

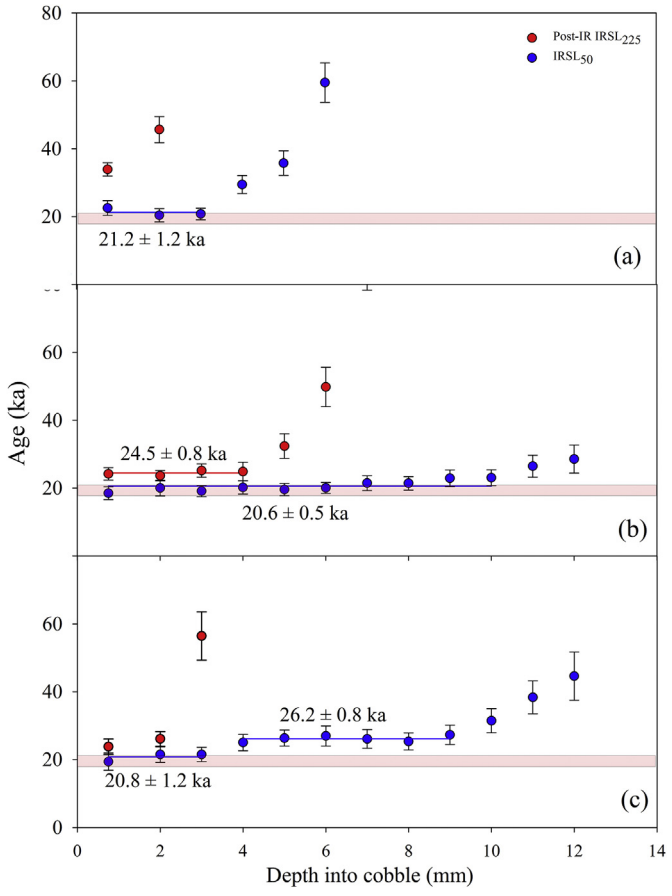

Fig. 9. Post-IR $IRSL_{225}$ (red) ages and fading-corrected $IRSL_{50}$ ages (blue) with depth into cobbles (a) ORS02-1, (b) ORS04-3, and (c) ORS04-1. The independent age control derived from Smedley et al. (2017b) and Chiverrell et al. (submitted) is also given in the light red shaded area (18.9 ± 1.0 ka to 20.3 ± 0.6 ka). (For interpretation of the references to colour in this figure legend, the reader is referred to the Web version of this article.)

The differences seen in the depth to which L_n/T_n ratios appear to be well bleached (Fig. 6) are reflected in the data in Fig. 9 when apparent ages are calculated for each slice. As expected, the $IRSL_{50}$ signal is seen to bleach to a greater depth into each of the three cobbles than the post-IR-$IRSL_{225}$ signal. For all three cobbles, slices from the outermost portion of each core give $IRSL_{50}$ ages which are consistent with one another. For cobble ORS02-1 (Fig. 9a) slices from the uppermost 2.8 mm (3 slices from each of 3 cores on the same cobble face) give an average fading-corrected $IRSL_{50}$ age of 21.2 ± 1.2 ka (n = 9 slices); for cobble ORS04-3 (Fig. 9b) the uppermost ~9 mm (10 slices from each of 3 cores) give a fading-corrected $IRSL_{50}$ age of 20.6 ± 0.5 ka (n = 27 slices, as 3 slices were lost at the base of one core); and the uppermost 3 slices of cobble ORS04-1 (Fig. 9c) give a fading-corrected $IRSL_{50}$ age of 20.8 ± 1.2 ka (n = 9 slices). These slices nearest the surface of these three cores (Fig. 9a–c) give ages that are similar to one another, yielding a mean age for the deposit of 20.7 ± 0.3 ka (n = 45 slices).

The post-IR $IRSL_{225}$ ages show a monotonic increase with depth into the core for two of the three samples (cobbles ORS02-1 and ORS04-1; Fig. 9a and c), and so it is not possible to be confident from these data alone that the surface post-IR $IRSL_{225}$ signals were bleached. The fading-corrected $IRSL_{50}$ ages show that cobble ORS04-3 is the clast that has been bleached to the greatest depth (>9 mm; Fig. 9b), and the post-IR $IRSL_{225}$ ages from the uppermost ~4 mm of this cobble are also consistent with one another, suggesting that this clast was well bleached at deposition. The mean post-IR $IRSL_{225}$ age for cobble ORS04-3 is 24.5 ± 0.8 ka (n = 9 slices), whilst the corresponding mean fading-corrected $IRSL_{50}$ age is significantly younger, being 20.6 ± 0.5 ka (n = 27 slices). These paired age determinations, measured for the same slices, do not agree with each other within two sigma uncertainties, and only the $IRSL_{50}$ age is in agreement with the independent age control for the site of 18.9 ± 1.0 to 20.3 ± 0.6 ka (Chiverrell et al., submitted; Smedley et al., 2017b). The disagreement between the $IRSL_{50}$ and post-IR $IRSL_{225}$ ages is intriguing. The consistency in the post-IR $IRSL_{225}$ ages with depth imply that although this signal is harder to bleach than the $IRSL_{50}$ signal, nevertheless it was uniformly reset to a depth of almost 4 mm at deposition (see also Fig. 6c). Some research has suggested that there could be an unbleachable component in the post-IR $IRSL_{225}$ signal, but the magnitude of this appears to be ~1–2 Gy (Thomsen et al., 2008; Smedley et al., 2015) and would equate to less than a few hundred years in the present study. It is also noteworthy that an overestimate of D_e was observed in the post-IR $IRSL_{225}$ signal dose-recovery experiment using a dose applied to a naturally-bleached cobble from the beach (32% overestimate, Table 2), though this effect was not seen when a sample was artificially bleached in the laboratory (Table 2). At present, the reason for the difference between the ages from the $IRSL_{50}$ and post-IR $IRSL_{225}$ signals is not known, but the greater sensitivity to daylight exposure of the $IRSL_{50}$ signal makes it the optimal signal for dating in this type of environment, and the fading-corrected $IRSL_{50}$ ages generated are shown to agree with the available independent age control.

In cobble ORS04-1 (Fig. 9c) the $IRSL_{50}$ ages are consistent for the three uppermost slices, a pattern similar to that seen in the other two sets of measurements in Fig. 9 (a & b). If the cobble records a single episode of sunlight exposure then one would expect the D_e (and apparent age) to increase monotonically below some point in the cobble. This is seen for cobble ORS02-1 (Fig. 9a) which rises steeply until the samples are in field saturation (as seen in Fig. 6c).

In contrast, the ages for cobble ORS04-1 rise to a second plateau (Fig. 9c), giving an average age of 26.2 ± 0.8 ka (n = 12 slices) from a depth of ~3.5–8.5 mm. The consistency in the age implies that the cobble had been bleached fully to a depth of ~8.5 mm at that time and then buried. Subsequently the cobble was moved a second time (re-worked), but this time only exposed for sufficient time such that the upper ~3 mm was fully bleached, and then deposited finally at 20.8 ± 1.2 ka. Since the depositional context in which this earlier event took place is not known, it is difficult to be confident of the palaeoenvironmental significance of this earlier resetting event. However, it is possible that this earlier event may relate to the advance of the Irish Sea Ice Stream, as modelled by Chiverrell et al. (2013) using the limited radiocarbon evidence available from the Irish Sea Basin.

The age of 20.7 ± 0.3 ka derived from the average of the fading-corrected $IRSL_{50}$ ages (n = 45 slices) from the 3 cobbles shown in Fig. 9 is almost identical to the revised retreat age (20.3 ± 0.6 ka; Smedley et al., 2017b) for the margin of the Irish Sea Ice Stream as it crossed the Isle of Anglesey ~70 km to the south of the study site, and implies that once the Irish Sea Ice Stream retreated past the pinning point formed by the Isle of Anglesey, recession then occurred very rapidly.

8. Conclusions

This paper examined the application of luminescence dating to cobbles from a glaciofluvial environment. The importance of careful sample site selection and of recording the orientation of cobbles was highlighted through the targeted sampling of bar-top lithofacies to maximise the likelihood of exposure to sunlight, which demonstrated that the up-orientated surfaces of the cobbles were the best-bleached on deposition, some to depths of up to 12 mm in granite. A procedure was developed to rapidly identify the best-bleached cobbles by measuring the L_n/T_n ratio of the surface rock slices from cobbles, without the need for further slicing or analysis of the deeper material drilled from the cobbles. The variable nature of the bleaching opportunities within a glaciofluvial deposit was demonstrated, with some cobbles giving a consistent value for age across several mm depth into the cobble implying that the luminescence signal had been fully-reset on deposition, whilst others showed little sign of resetting at deposition, giving a rapid increase in apparent age with depth from the surface. In accordance with studies on sand-sized grains, the $IRSL_{50}$ signal is reset more rapidly and to a greater depth than the post-IR $IRSL_{225}$ signal, with only one cobble showing evidence of the post-IR $IRSL_{225}$ signal being well-bleached on deposition. Only cobbles offer this clear assessment of whether the luminescence signal was completely reset at deposition, thereby avoiding the need for application of the complex statistical models used when dating sand-sized sediment grains in similar glaciofluvial settings. A further advantage to working with cobbles is that the dose rate is much less sensitive to variations in water content than is the dose to sand-sized grains. This is clearly advantageous in glacial or glaciofluvial settings where water contents can reach high values, and can vary over the time since deposition. At a depth of 2 mm or more into the surface, more than 90% of the dose rate arises from the cobble itself rather than its surroundings, and this dose rate is not influenced by water in the surrounding sediment.

The fading-corrected $IRSL_{50}$ ages from three well-bleached cobble faces yield reproducible ages, giving a mean age of 20.7 ± 0.3 ka (n = 45 slices), in agreement with independent age control provided by Chiverrell et al. (submitted) and Smedley et al. (2017b). In one of the well-bleached cobbles, the $IRSL_{50}$ data shows evidence of two discrete exposure events and this single clast potentially records both the advance of the Irish Sea ice stream at 26.2 ± 0.8 ka, as well as its retreat at 20.7 ± 0.3 ka, providing further constraint on the pace of rapid ice marginal retreat in the northern Irish Sea basin. This study is the first to successfully date glaciofluvial sediments using cobbles, demonstrating a number of advantages of working with cobbles as a substrate for dating and highlighting the potential for the use of cobbles in future dating studies of glacial sediments.

Acknowledgments

This paper was supported by a Natural Environment Research Council consortium grant (BRITICE-CHRONO NE/J008672/1). We thank Professor Andrew Murray and Vicki Hansen at the Nordic Laboratory for Luminescence Dating for gamma irradiating rock slices for calibration. GTHJ thanks Aberystwyth University for a DCDS Postgraduate Scholarship, DGES for contributing to fieldwork costs, and the QRA for a conference award to allow the work to be presented at the International Luminescence and Electron Spin Resonance dating conference in 2017. We also thank Dr Rachel Smedley for assistance in the field and Miss Hollie Wynne for assistance in the laboratory. Two anonymous referees are thanked for their comments which improved this paper.

Appendix A. Supplementary data

Supplementary data related to this article can be found at https://doi.org/10.1016/j.quascirev.2018.05.036.

References

Aitken, M.J., 1985. Thermoluminescence Dating. Academic press.
Auclair, M., Lamothe, M., Huot, S., 2003. Measurement of anomalous fading for feldspar IRSL using SAR. Radiat. Meas. 37, 487–492.
Bøtter-Jensen, L., Mejdahl, V., 1988. Assessment of beta dose-rate using a GM multicounter system. Nucl. Tracks Radiat. Meas. 14, 187–191.
Bøtter-Jensen, L., Andersen, C.E., Duller, G.A.T., Murray, A.S., 2003. Developments in radiation, stimulation and observation facilities in luminescence measurements. Radiat. Meas. 37, 535–541.
Buylaert, J.P., Murray, A.S., Thomsen, K.J., Jain, M., 2009. Testing the potential of an elevated temperature IRSL signal from feldspar. Radiat. Meas. 44, 560–565.
Chiverrell, R.C., Thrasher, I.M., Thomas, G.S., Lang, A., Scourse, J.D., van Landeghem, K.J.J., McCarroll, D., Clark, C.D., O'Cofaigh, C., Evans, D.J.A., Ballantyne, C.K., 2013. Bayesian modelling the retreat of the Irish Sea ice stream. J. Quat. Sci. 28, 200–209.
Chiverrell, R.C., Smedley, R.K., Small, D., Ballantyne, C.K., Burke, M.J., Callard, L., Clark, C., Duller, G.A.T., Evans, D.J.A., Fabel, D., Van Landeghem, K.J.J., Livingstone, S., O Cofaigh, C., Thomas, G.S.P., Roberts, D., Saher, M., Scourse, J.D., Wilson, P., Submitted. Ice margin oscillations during deglaciation of the northern Irish Sea basin. J. Quat. Sci..
Colarossi, D., Duller, G.A.T., Roberts, H.M., Tooth, S., Lyons, R., 2015. Comparison of paired quartz OSL and feldspar post-IR IRSL dose distributions in poorly bleached fluvial sediments from South Africa. Quat. Geochronol. 30, 233–238.
Duller, G.A.T., 2004. Luminescence dating of Quaternary sediments: recent advances. J. Quat. Sci. 19, 183–192.
Duller, G.A.T., 2008. Single grain optical dating of Quaternary sediments: why aliquot size matters in luminescence dating. Boreas 37, 589–612.
Freiesleben, T., Sohbati, R., Murray, A., Jain, M., Al Khasawneh, S., Hvidt, S., Jakobsen, B., 2015. Mathematical model quantifies multiple daylight exposure and burial events for rock surfaces using luminescence dating. Radiat. Meas. 81, 16–22.
Galbraith, R.F., Roberts, R.G., 2012. Statistical aspects of equivalent dose and error calculation and display in OSL dating: an overview and some recommendations. Quat. Geochronol. 11, 1–27.
Galbraith, R.F., Roberts, R.G., Laslett, G.M., Yoshida, H., Olley, J.M., 1999. Optical dating of single and multiple grains of quartz from Jinmium rock shelter, northern Australia: Part I, experimental design and statistical models. Archaeometry 41, 339–364.
Guérin, G., Mercier, N., Adamiec, G., 2011. Dose-rate conversion factors: update. Ancient TL 29, 5–8.
Habermann, J., Schilles, T., Kalchgruber, R., Wagner, G.A., 2000. Steps towards surface dating using luminescence. Radiat. Meas. 32, 847–851.
Huntley, D.J., Baril, M.R., 1997. The K content of the K-feldspars being measured in optical dating or in thermoluminescence dating. Ancient TL 15, 11–13.
Huntley, D.J., Lamothe, M., 2001. Ubiquity of anomalous fading in K-feldspars and the measurement and correction for it in optical dating. Can. J. Earth Sci. 38,

1093–1106.
Ou, X.J., Duller, G.A.T., Roberts, H.M., Zhou, S.Z., Lai, Z.P., Chen, R., Chen, R., Zeng, L., 2015. Single grain optically stimulated luminescence dating of glacial sediments from the Baiyu Valley, southeastern Tibet. Quat. Geochronol. 30, 314–319.
Polikreti, K., Michael, C.T., Maniatis, Y., 2002. Authenticating marble sculpture with thermoluminescence. Ancient TL 20, 11–18.
Prescott, J.R., Hutton, J.T., 1994. Cosmic ray contributions to dose rates for luminescence and ESR dating: large depths and long-term time variations. Radiat. Meas. 23, 497–500.
Rees-Jones, J., 1995. Optical dating of young sediments using fine-grain quartz. Ancient TL 13, 9–14.
Simkins, L.M., DeWitt, R., Simms, A.R., Briggs, S., Shapiro, R.S., 2016. Investigation of optically stimulated luminescence behavior of quartz from crystalline rock surfaces: a look forward. Quat. Geochronol. 36, 161–173.
Small, D., Smedley, R.K., Chiverrell, R.C., Scourse, J.D., O Cofaigh, C., Duller, G.A.T., McCarron, S., Burke, M.J., Evans, D.J.A., Fabel, D., Gheorghiu, D.M., Thomas, G.S.P., Xu, S., Clark, C.D., 2018. Trough geometry was a greater influence than climate-ocean forcing in regulating retreat of the marine-based Irish-Sea Ice Stream. Geol. Soc. Am. Bull. Accepted: https://doi.org/10.1130/B31852.1.
Smedley, R.K., Duller, G.A.T., Roberts, H.M., 2015. Bleaching of the post-IR IRSL signal from individual grains of K-feldspar: implications for single-grain dating. Radiat. Meas. 79, 33–42.
Smedley, R.K., Glasser, N.F., Duller, G.A.T., 2016. Luminescence dating of glacial advances at Lago Buenos Aires (~46 °S), Patagonia. Quat. Sci. Rev. 134, 59–73.
Smedley, R.K., Scourse, J.D., Small, D., Hiemstra, J.F., Duller, G.A.T., Bateman, M.D., Burke, M.J., Chiverrell, R.C., Clark, C.D., Davies, S.M., Fabel, D., Gheorghiu, D.M., McCarroll, D., Medialdea, A., Xu, S., 2017a. New age constraints for the limit of the British–Irish ice sheet on the Isles of Scilly. J. Quat. Sci. 32, 48–62.
Smedley, R.K., Chiverrell, R.C., Ballantyne, C.K., Burke, M.J., Clark, C.D., Duller, G.A.T., Fabel, D., McCarroll, D., Scourse, J.D., Small, D., Thomas, D.S.G., 2017b. Internal dynamics condition centennial-scale oscillations in marine-based ice-stream retreat. Geology 45, 787–790.
Sohbati, R., Murray, A.S., Buylaert, J.P., Almeida, N.A., Cunha, P.P., 2012. Optically stimulated luminescence (OSL) dating of quartzite cobbles from the Tapada do Montinho archaeological site (east-central Portugal). Boreas 41, 452–462.
Sohbati, R., Murray, A.S., Porat, N., Jain, M., Avner, U., 2015. Age of a prehistoric "Rodedian" cult site constrained by sediment and rock surface luminescence dating techniques. Quat. Geochronol. 30, 90–99.
Svendsen, J.I., Alexanderson, H., Astakhov, V.I., Demidov, I., Dowdeswell, J.A., Funder, S., Gataullin, V., Henriksen, M., Hjort, C., Houmark-Nielsen, M., Hubberten, H.W., Ingolfsson, O., Jakobsson, M., Kjaer, K.H., Larsen, E., Lokrantz, H., Lunkka, J.P., Lysa, A., Mangerud, J., Matiouchkov, A., Murray, A., Moller, P., Niessen, F., Nikolskaya, O., Polyak, L., Saarnisto, M., Siegert, C., Siegert, M.J., Spielhagen, R.F., Stein, R., 2004. Late Quaternary ice sheet history of northern Eurasia. Quat. Sci. Rev. 23, 1229–1271.
Thiel, C., Buylaert, J.P., Murray, A., Terhorst, B., Hofer, I., Tsukamoto, S., Frechen, M., 2011. Luminescence dating of the Stratzing loess profile (Austria)–Testing the potential of an elevated temperature post-IR IRSL protocol. Quat. Int. 234, 23–31.
Thomas, G.S.P., Connaughton, M., Dackombe, R.V., 1985. Facies variation in a Late Pleistocene supraglacial outwash sandur from the Isle of Man. Geol. J. 20, 193–213.
Thomas, G.S.P., Chiverrell, R.C., Huddart, D., Long, D., Roberts, D., 2006a. The ice age. In: Chiverrell, R.C., Thomas, G.S.P. (Eds.), A New History of the Isle of Man: the Evolution of the Natural Landscape. Liverpool University Press, Liverpool, pp. 100–150.
Thomas, P.J., Murray, A.S., Kjaer, K.H., Funder, S., Larsen, E., 2006b. Optically stimulated luminescence (OSL) dating of glacial sediments from Arctic Russia - depositional bleaching and methodological aspects. Boreas 35, 587–599.
Thomsen, K.J., Murray, A.S., Jain, M., Bøtter-Jensen, L., 2008. Laboratory fading rates of various luminescence signals from feldspar-rich sediment extracts. Radiat. Meas. 43, 1474–1486.
Thrasher, I.M., Mauz, B., Chiverrell, R.C., Lang, A., Thomas, G.S.P., 2009. Testing an approach to OSL dating of Late Devensian glaciofluvial sediments of the British Isles. J. Quat. Sci. 24, 785–801.
Vafiadou, A., Murray, A.S., Liritzis, I., 2007. Optically stimulated luminescence (OSL) dating investigations of rock and underlying soil from three case studies. J. Archaeol. Sci. 34, 1659–1669.